EAI Endorsed Transactions
on Energy Web
Research Article EAI.EU

Analysis of the Impact of Active Power Recovery Rate of Wind Farms on Power System Transient Stability

Hongxuan Zhang[1],Peng Zhou[2],Jianxin Zhang[1],Qing Gao[1],Tuo Jiang[1],Huanhuan Yang[1],Yanzhe Cheng[2,*]

[1]China Southern Power Grid Dispatching and Control Center, Guangzhou, Guangdong, China
[2]School of Electrical Engineering, Northeast Electric Power University, Jilin, Jilin, China

Abstract

INTRODUCTION: The post-fault active-power recovery of DFIG wind farms strongly influences transient-stability assessment, yet conventional equivalent models fail to capture variations in recovery rate during LVRT. This paper proposes an equivalent modeling method that embeds optimized recovery characteristics. First, the post-fault recovery behavior is analyzed. A single-machine equivalent with an optimized recovery rate and a multi-machine equivalent representing piecewise recovery are then developed. Differences from a detailed wind-farm model are quantified using error indices and curve similarity, and impacts on simulation credibility are assessed. Results show the proposed models better reproduce recovery dynamics and improve transient-stability accuracy.
OBJECTIVES: characterize post-fault active-power recovery in wind farms, develop accurate equivalents for the restoration stage, and reveal how integration models affect power-system transient stability.
METHODS: Single-machine and multi-machine wind-farm equivalencing with optimized active-power recovery (and turbine time constants), plus the transient energy-function method.
RESULTS: Compared with conventional methods reported in the literature, the proposed wind farm equivalencing methods reduce the relative error of model equivalencing from 18.84% to 9.49% and 3.70%, respectively. In addition, the relative error in transient stability analysis is reduced from 22.68% to 9.19% and 2.35%, respectively.
CONCLUSION AND SIGNIFICANCE: To establish a high-accuracy equivalent model of the wind farm, thereby providing a reliable modeling basis for transient stability analysis of power systems with wind power integration.

Keywords: Power systems; active power recovery rate; transient stability; wind farm equivalent model

Received on 09 April 2026, accepted on 12 May 2026, published on 18 May 2026

doi: 10.4108/ew.12533

1. Introduction

As wind power is being deployed on a much larger scale in contemporary power systems, the share of wind generation in the overall energy mix has steadily increased, which has substantially reshaped fault response characteristics in areas with high renewable penetration [1]. Accordingly, transient stability issues have become more prominent, highlighting the need to examine how extensive wind power integration influences rotor angle transient stability. Under the "dual carbon" strategy, the sustained expansion of renewable installed capacity has also led to a decline in the equivalent inertia of power systems. When severe disturbances occur, the reduced inertia may even cause large scale tripping of renewable generation units. Moreover, cascading disturbances further complicate the dynamic behavior of the system during the

*Corresponding author. Email: 2202300092@neepu.edu.cn

transient process, which makes accurate evaluation of transient rotor angle stability increasingly difficult [2].

Doubly-Fed Induction Generator (DFIG)-based wind turbines continue to be widely used in modern power systems, and extensive research has been conducted on their transient characteristics and corresponding control schemes [3]-[7]. Different from traditional synchronous generators, wind turbines generally exhibit unique dynamic responses under grid fault conditions. Especially during LVRT, a lack of sufficient active power support from wind turbines may worsen the transient stability of synchronous generators, thereby reducing system stability margins. For both individual turbines and equivalent wind farm representations, the rate of recovery in the post fault stage is an important LVRT related indicator. It characterizes the ability of wind generation units to regain active power output after fault removal and is therefore related to the secure operation of the interconnected grid. In engineering oriented time domain analysis, wind farms are usually simplified into several equivalent turbine models to reproduce their collective dynamic response. As a result, the effectiveness of the adopted equivalent model largely affects the credibility of simulation results and the accuracy of transient stability analysis [8]. On this basis, a transient wind farm model capable of accurately representing active power recovery behavior is essential for studying the impact of wind farm integration on rotor angle transient stability.

Based on the number of equivalent units adopted, wind farm equivalencing methods generally inclued single machine and multi machine approaches. In a single machine equivalent approache, using one equivalent generator to represent the output behavior of an entire DFIG-based wind farm, which gives this method a high degree of simplification. Because the equivalent parameters are commonly determined by weighting turbine capacity, this approach is also referred to as the capacity weighting method [9]-[10]. To achieve higher equivalencing accuracy, some researchers have developed multi-machine equivalent models in which turbines are grouped according to state variables such as wind speed, active power, and voltage under both steady-state and fault conditions [11].

Several studies have also taken the power recovery rate after fault clearing into account and investigated the sources of equivalence error during the recovery process, using wind speed differences as the basis for turbine classification [12]. In addition, the LVRT control characteristics of DFIGs have been incorporated into the equivalencing procedure in some existing work. More specifically, once a DFIG operates within the LVRT region, the crowbar switching strategy is determined by the severity of the fault: during deep voltage dips the crowbar is triggered, whereas prior to its activation the short-circuit current is indirectly controlled through the rotor-side converter to meet grid-code requirements [13]. Zuo et al. proposed a two-stage clustering strategy in which turbines were first roughly classified according to active power and then regrouped through a clustering algorithm, thereby improving the equivalent model accuracy of the wind farm [14]. Furthermore, since protection status may also influence short-circuit current characteristics, some studies have employed the post fault limiter state as an additional clustering index [15].

Beyond model equivalencing, a number of methods have been developed for transient stability assessment. Matavalam et al. combined data driven techniques with time-domain simulation and designed an optimization algorithm for transient stability analysis in power systems [16]. To reduce the effect of misclassified samples in deep-learning based training datasets, Bogodorova et al. proposed a probabilistic metric that enhances assessment accuracy [17]. Keivanimehr et al. introduced a transient stability index and integrated it with the extended equal area criterion, making real time transient stability evaluation possible [18]. Peng et al. developed a method that combines Taylor expansion with adaptively adjusted numerical integration and applied it to large-scale simulations of transient stability in complex power systems. Their results indicate that the proposed algorithm can markedly reduce computational cost while improving analysis efficiency [19]. Brik et al. investigated the impact of wind and photovoltaic (PV) integration on power-system transient stability and showed that, under short-circuit fault conditions, dynamically regulating wind and PV output can improve transient stability performance [20].

Tang et al. modeled the DFIG as an equivalent constant-power source before the fault and after fault clearance, and derived the corresponding conditions under which this simplification is applicable. However, that approach assumes that active power recovers instantaneously once the fault is removed [21]. In actual DFIG based wind farms, such an assumption may introduce an unrealistically strong power disturbance to the grid. Therefore, representing post-fault wind turbines as constant power sources may be inadequate in scenarios with stringent accuracy requirements. For this reason, the power recovery process of wind turbines and wind farms should be explicitly considered to improve the equivalencing accuracy of wind farm models.

This study aims to accurately describe the dynamic power recovery characteristics of wind farms after fault clearing, construct high fidelity equivalent models for the active-power restoration stage, and clarify the mechanism by which wind farm integration models affect power-system transient stability. To achieve these objectives, three main methods are adopted: a wind farm single-machine equivalencing approach based on the optimal active power recovery rate, a wind farm multi machine equivalencing approach that considers both the optimal active power recovery rate and wind-turbine recovery time constants, and the transient energy function method. In comparison with conventional approaches reported in previous studies, the proposed wind farm equivalencing methods decrease the relative equivalencing error from 18.84% to 9.49% and 3.70%, respectively. The equivalent model errors of the wind farm were reduced by 9.35% and

15.14%, corresponding to decreases of 49.6% and 80.4%, respectively, indicating a significant reduction in error. Meanwhile, the relative error in transient stability analysis is reduced from 22.68% to 9.19% and 2.35%, respectively. The transient stability assessment indices decreased by 13.49% and 20.43%, corresponding to reductions of 59.5% and 90.1%, respectively, indicating a marked improvement in accuracy. On this basis, the paper further examines how recovery dynamics of wind turbines influence transient stability in power systems, develops an analytical model, and systematically assesses the impact of the wind farm recovery rate.

2. Research Approach

2.1. Transient Stability Analysis Method

The transient stability mechanism considered in this study is derived using the DC power flow approximation together with the classical model. In the analytical derivation, the electromagnetic power dynamics of synchronous generators are neglected. To simplify the analysis and make the mechanism more transparent, a single machine infinite bus (SMIB) system is employed. A finite-capacity generator is connected to an infinite-bus power system through a double-circuit transmission line. In Fig. 1, the output power of the finite-capacity generator is assumed to be P. The infinite bus is represented by a generator with constant voltage and zero internal impedance, and the impedance of each circuit of the double-circuit transmission line is assumed to be x. Figure 1. shows the schematic diagram of the system wiring.

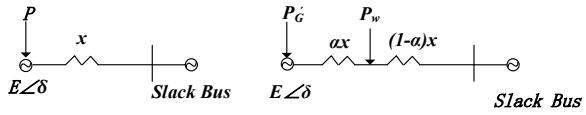

(a)Before wind power integration (b) After wind power integration

Figure 1 System configuration before and after wind power integration

With the electromagnetic power of the synchronous generator neglected, the rotor angular velocity and power angle in the SMIB system are given by [22]:

$$\begin{cases} \Delta\omega = \frac{P_m}{M} t \\ \delta = \frac{\omega_0 P_m}{M} t^2 + \delta_0 \end{cases} \quad (1)$$

Considering the synchronous generator in the SMIB system, the following expression is obtained:

$$\frac{d^2\delta}{dt^2} = \frac{\omega_0}{M}(P_m - P_e) \quad (2)$$

In the equation, M denotes the inertia constant of the synchronous generator; ω is the angular frequency; δ is the rotor angle; P_m is the mechanical input power; and P_e is the electromagnetic power, namely the electrical output power, of the synchronous generator.

Let represent the variation in the angle of the synchronous generator prior to and following the integration of wind power, which indicates the influence of the incorporation on stability. If an increase in the rotor angle occurs after integrating wind power, suggesting a decline in transient stability. Conversely, if , a decrease in the rotor angle follows the wind power integration, indicating an enhancement in transient stability[23].

By comparing the rotor motion equations of the synchronous generator before and after wind power integration, the following difference equation can be obtained:

$$\frac{d^2\Delta\delta}{dt^2} = \frac{d^2\delta'}{dt^2} - \frac{d^2\delta}{dt^2} = \frac{\omega_0}{M}\left(P_m' - P_e'\right) - \frac{\omega_0}{M}\left(P_m - P_e\right) \quad (3)$$

In this paper, the superscript denotes the value of a physical quantity after wind power integration. If the mechanical input power P_m and electromagnetic power P_e of the synchronous generator can be determined for the fault on and post fault periods in both the pre-integration and post integration scenarios, the changes in the acceleration and deceleration areas induced by wind power integration can be estimated, thereby enabling an analysis of its impact on the system's transient stability.

2.2 Validity of the Power Injection Model for Doubly-Fed Wind Farms

This study focuses on DFIG-based wind turbine generators operating under maximum power point tracking (MPPT) without any virtual inertia emulation. For such DFIGs, rotor angle stability is not considered herein. Under standard operating conditions, the reference for active power is established at the highest aerodynamic power that can be harnessed given the current wind speed, enabling near optimal wind energy utilization. With stator voltage oriented vector control (SVOC) applied to the rotor side converter (RSC), both active and reactive power can be independently controlled. Accordingly, under this control framework, the turbine active power is given by:

$$P_s = \frac{3}{2}\frac{L_m}{L_s} U_s i_{rd} \quad (4)$$

The equation above illustrates that the active power of a DFIG is directly related to both the stator voltage and the d-axis component of the rotor current. Generally, the time constant for the current control loop is in the range of several tens of milliseconds, which is much smaller than the timescale of active power recovery after fault clearance. Therefore, this paper mainly considers variations in the stator voltage. In the typical functioning of a DFIG, the stator voltage is maintained at a constant level. This characteristic allows for the turbine to be effectively represented as a constant power source under normal operational conditions. However, the scenario changes significantly during a fault period. In such instances, the output of the DFIG is constrained, leading to a situation

where the electromagnetic power generated is nearly zero. This reduction in power output highlights the vulnerabilities of the system during fault conditions, underscoring the need for effective management strategies to handle operational disruptions.

During the stage of active power restoration following a fault, the output from the turbine is limited by the ramp rate. As a result, the active power cannot immediately return to its steady-state value prior to the fault; rather, it increases gradually at a specified rate until the operation point before the fault is attained. Simulations conducted in the time domain with a constant power factor control produce the corresponding curves for active and reactive power responses, as shown in Fig. 2.During this interval, the active power of DFIG is given by:

$$P_w = k(t - t_c) + P_f \tag{5}$$

In the active power recovery phase, each DFIG-based wind turbine exhibits a recovery of active power at a specific rate, denoted as k. When considering a wind farm that comprises multiple turbines, the overall recovery rate can be determined by aggregating the individual recovery rates of all turbines that are currently engaged in the process of active power recovery. This means that the total recovery rate of the entire wind farm is the collective sum of the recovery rates of each turbine that is still in the active recovery mode. Assuming identical recovery rates for all DFIGs within the same wind farm, differences in individual turbine output power result in different recovery completion times. As each turbine in the wind farm progressively completes its recovery phase and transitions out of this state, there is a noticeable decline in the overall rate of the farm. This gradual decrease highlights a distinct pattern within the active power recovery process, which can be characterized as piecewise linear. Furthermore, the simulation results visually represented in Figure 2 illustrate the active power curve of the wind farm when operating under a constant power factor. This visualization serves to effectively demonstrate the behavior of the active power recovery process during turbine recovery, confirms the validity of modeling the wind farm as a piecewise linear active power injection model.

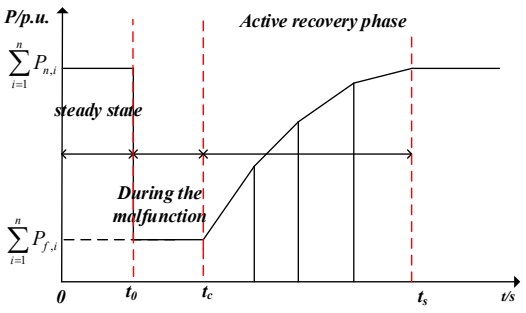

Figure 2. Active power recovery curve of the wind farm

Figure 2 illustrates the variation process of the wind farm's active power under external disturbances. The system is initially operating in a steady state. After the disturbance occurs, its performance rapidly declines to a lower level; subsequently, during the recovery stage, it gradually rises through multiple recovery-rate stages and eventually returns to the steady state.

3. Derivation of Transient Stability Mechanism

This paper derives the transient stability mechanism based on the DC power flow model and the classical second order generator model. It is assumed that, after DFIG-based wind turbines are integrated into the system, the active load remains unchanged, while the synchronous generators reduce their corresponding active power output accordingly.

In the SMIB system, with the infinite bus taken as the slack bus, the steady state power angle of the synchronous generator before wind power integration is given by [24]:

$$\delta_0 = Px \tag{6}$$

During the fault period, the electromagnetic power is approximately zero, and the resulting unbalanced power of the synchronous generator is given by:

$$P_m - P_e = P \tag{7}$$

The dynamic evolution of the synchronous generator rotor angle can be further characterized by its second order derivative, which reflects the acceleration or deceleration behavior of the rotor under the influence of power imbalance. This quantity is governed by the swing equation and takes a crucial role in describing the transient response of the synchronous machine. Accordingly, the second derivative of the synchronous generator power angle is given by:

$$\frac{d^2\delta}{dt^2} = \frac{\omega_0}{M}(P_m - P_e) = \frac{\omega_0}{M}P > 0 \tag{8}$$

Following fault clearing, the synchronous generator operates in the post-fault stage, where its dynamic response is determined by the mismatch between mechanical input power and electrical output power. This mismatch, referred to as the unbalanced power, directly influences rotor acceleration and the transient stability. Therefore, the unbalanced power of the synchronous generator in the post-fault period can be written as:

$$P_m - P_e = P - \frac{\delta}{x_{II}} \tag{9}$$

The second derivative of the rotor angle is given by:

$$\frac{d^2\delta}{dt^2} = \frac{\omega_0}{M}(P_m - P_e) = \frac{\omega_0}{M}\left(P - \frac{\delta}{x_{II}}\right) < 0 \tag{10}$$

After the DFIG-based wind farm is connected, let P_w represent its total active power output. To ensure the overall active power balance of the system, the active power supplied by the synchronous generator can therefore be expressed as:

$$P_G^{'} = P - P_w \tag{11}$$

Following the integration of wind power into the system, the steady-state power angle of the synchronous generator is no longer determined solely by the conventional generation-load balance, but is also affected by the active power contribution of the wind farm. Under this condition, the operating point of the synchronous machine shifts accordingly, and its steady state power angle can be expressed as:

$$\delta_0^{'} = P_G{}'x + P_w(1-\alpha)x \tag{12}$$

Considering the wind turbine integration, the pre-fault steady-state change in the synchronous machine power angle is given by:

$$\Delta\delta = \delta_0^{'} - \delta_0 = P_G{}'x + P_w(1-\alpha)x - Px = -\alpha P_w x \tag{13}$$

After the wind power incorporated, the power imbalance produced by the synchronous generator is given by:

$$P_m^{'} - P_e^{'} = P_G{}' = P - P_w \tag{14}$$

The second derivative of the synchronous machine power angle is given by:

$$\frac{d^2\delta^{'}}{dt^2} = \frac{\omega_0}{M}\left(P_m^{'} - P_e^{'}\right) = \frac{\omega_0}{M}\left(P - P_w\right) \tag{15}$$

Once the wind turbine is connected, the alteration in the acceleration of the synchronous generator rotor angle during the fault is given by:

$$\frac{d^2\Delta\delta}{dt^2} = \frac{d^2\delta^{'}}{dt^2} - \frac{d^2\delta}{dt^2} = \frac{\omega_0}{M}\left(P - P_w\right) - \frac{\omega_0}{M}P = -\frac{\omega_0}{M}P_w \tag{16}$$

The above equation that, after wind power is integrated, if the wind farm produces no output during the fault period, the synchronous machine power imbalance and the second derivative of its power angle during the fault remain the same as those before wind power integration. If the wind turbine delivers a certain amount of power during the fault, the accelerating area of the synchronous machine decreases.

After the fault is cleared, the power imbalance of the synchronous generator is given by:

$$P_m^{'} - P_e^{'} = P - \left(\frac{\delta^{'}}{x_{II}} + \alpha P_{\mathrm{w}}\right) \tag{17}$$

The second derivative of the synchronous machine power angle is given by:

$$\frac{d^2\delta^{'}}{dt^2} = \frac{\omega_0}{M}\left(P_m^{'} - P_e^{'}\right) = \frac{\omega_0}{M}\left[P - \left(\frac{\delta^{'}}{x_{II}} + \alpha P_{\mathrm{w}}\right)\right] \tag{18}$$

After fault clearance, the variation in the second derivative of the synchronous machine rotor angle due to wind power integration is given by:

$$\begin{aligned}\frac{d^2\Delta\delta}{dt^2} &= \frac{d^2\delta^{'}}{dt^2} - \frac{d^2\delta}{dt^2} \\ &= \frac{\omega_0}{M}\left[P - \left(\frac{\delta^{'}}{x_{II}} + \alpha P_{\mathrm{w}}\right)\right] - \frac{\omega_0}{M}\left(P - \frac{\delta}{x_{II}}\right) \\ &= -\frac{\omega_0}{M}\alpha P_{\mathrm{w}} < 0\end{aligned} \tag{19}$$

Under the premise that wind farms replace conventional thermal power units on an equivalent basis, the transient stability of the power system with wind power integration is determined by two factors: the characteristics of synchronous generators and the characteristics of wind power. Specifically, the characteristics of synchronous generators refer to the generator inertia, while the characteristics of wind power mainly include the point of wind power integration and the installed wind power capacity.

Therefore, if the synchronous generator reduces its output after wind power is integrated, wind power integration has a positive effect on the system's transient stability. Moreover, the larger the wind power output and the farther the wind farm interconnection point is from the synchronous generator, the more beneficial the impact on transient stability.

4. Transient Stability Analysis

In the current body of research regarding the influence of integrating DFIGs wind farms on the transient stability of synchronous generators, wind farms are typically modeled as constant power sources. This assumption is valid during normal pre-fault operation and for a short period after fault clearance. However, during the active power recovery stage following fault clearance, modeling doubly fed induction generators simply as constant power sources may lead to an optimistic estimate of the system decelerating area, and consequently to an overestimation of the transient stability.

Existing studies typically model a wind farm after fault clearance as a power source with either constant slope recovery or multi segment slope recovery, however, the impact of the power recovery characteristics of the wind farm on the transient stability of the system has not been comprehensively studied.. Therefore, this section analyzes the accuracy of using a single wind turbine with constant slope recovery to represent the dynamic behavior of a wind farm during the active power recovery stage, and quantitatively evaluates the impact of employing a constant slope recovery model for the wind farm on transient stability assessment, compared with a model which reflects the actual active power recovery rate.

4.1 Analysis of the Impact Mechanism of Recovery Rate on System Transient Stability

Once the wind power is integrated, the power angle at a steady state of the synchronous machine is given by [25]:

$$P_{w,1} = k(t - t_c) + P_f \tag{20}$$

For an actual wind farm comprising n units, assume that the units are indexed from 1 to n in ascending order of active power output. At the considered instant, the first j units have completed active power recovery, whereas unit j+1 and the remaining units are still recovering. Accordingly, the active power reference is given by:

$$P_{w,real}=\begin{cases}\left(\sum_{i=1}^{n}k_i\right)(t-t_c)+\sum_{i=1}^{n}P_{f,i}, t_c<t<t_1\\ \sum_{i=1}^{j}P_{n,i}+\left(\sum_{i=j+1}^{n}k_i\right)(t-t_c)+\sum_{i=1}^{n}P_{f,i}, t_1<t<t_s\\ \sum_{i=1}^{n}P_{n,i}+\sum_{i=1}^{n}P_{f,i}, t>t_s\end{cases} \quad (21)$$

Substituting (20) and (21) into (19), respectively, yields:

$$\left.\frac{d^2\Delta\delta}{dt^2}\right|_1=-\frac{\omega_0}{M}\alpha P_{w,1}=-\frac{\omega_0}{M}\alpha\left[k(t-t_c)+P_f\right] \quad (22)$$

$$\left.\frac{d^2\Delta\delta}{dt^2}\right|_{real}=-\frac{\omega_0}{M}\alpha P_{w,real} \quad (23)$$

Equation (22) gives the second derivative of the synchronous generator rotor angle when large-scale wind power is represented by an equivalent single turbine model, whereas equation (23) gives the second derivative of the rotor angle when the actual wind farm model is adopted.

Subtracting (23) from (22) gives:

$$\left.\frac{d^2\Delta\delta}{dt^2}\right|_1-\left.\frac{d^2\Delta\delta}{dt^2}\right|_{real}=-\frac{\omega_0}{M}\alpha\left(P_{w,1}-P_{w,real}\right)<0 \quad (24)$$

Equation (24) indicates that, compared with an actual wind farm, representing wind power integration using a single machine equivalent model yields a smaller second derivative of the synchronous generator rotor angle after fault clearance, thereby resulting in a larger deceleration area. Consequently, applying the single machine model in transient stability analysis tends to overestimate system transient stability. The accuracy of transient stability assessment is also affected by two categories of factors. The first is the characteristics of synchronous generators, mainly including generator inertia; the second is the characteristics of wind power, mainly including the point of wind power integration and the capacity of wind power that equivalently replaces conventional thermal power units. Moreover, as the electrical distance between the interconnection point and the synchronous generator increases, this gap widens, leading to greater overestimation of system transient stability.

4.2 Quantitative Evaluation Based on the Optimal Recovery Rate

The previous section elucidated the mechanism by which the single machine active power recovery rate model affects transient stability assessment. Building on this, this section develops a quantitative index system to evaluate how different wind turbine recovery rate models influence transient stability evaluation. In particular, it quantifies the impact on transient stability assessment of using a fixed slope recovery model for the wind farm instead of a model that captures the actual active power recovery rate.

Based on the study of actual wind farm output in this paper, the optimal recovery rate of the single machine equivalent model for a wind farm is proposed. It is defined as the recovery rate of a single machine equivalent model at which its output during the wind farm recovery process is closest to the actual output of the wind farm.

This paper proposes an absolute error index, defined as the difference in the second derivative of the synchronous generator rotor angle between the single machine representation of wind power and the actual wind farm model. The index is used to quantify the degree to which the deceleration area is overestimated when the wind farm is modeled using a single machine equivalent rather than its actual configuration.

$$\eta_1=\left|\left.\frac{d^2\Delta\delta}{dt^2}\right|_1-\left.\frac{d^2\Delta\delta}{dt^2}\right|_{real}\right|=\frac{\omega_0}{M}\alpha\left(P_{w,1}-P_{w,real}\right) \quad (25)$$

Due to the DFIG output characteristics, this index may take negative values. It quantitatively characterizes the impact of representing wind power integration with a single machine model on the deceleration area of synchronous generators. Its value is determined by the synchronous generator characteristics, the wind power interconnection location, and the difference in active power output between the single machine model and the actual wind farm. A smaller value indicates a larger deviation in the calculated deceleration area of the synchronous generator, whereas a larger value indicates a smaller deviation. If a multi machine equivalent model is used for the wind farm, the index can be extended by replacing the active power output expression during the recovery stage with the corresponding multi machine expression, enabling analysis of how the multi machine representation affects system transient stability.

Relative error index: It is defined as the ratio of the difference between the second derivative of the synchronous generator rotor angle obtained using the single machine wind power model and that obtained using the actual wind farm model to the maxi mum value of the second derivative of the synchronous generator rotor angle under the single machine wind power model.

$$\eta_2=\frac{\left.\frac{d^2\Delta\delta}{dt^2}\right|_1-\left.\frac{d^2\Delta\delta}{dt^2}\right|_{real}}{\left.\frac{d^2\Delta\delta}{dt^2}\right|_{1,\,Max}}=\frac{-\frac{\omega_0}{M}\alpha\left(P_{w,1}-P_{w,real}\right)}{-\frac{\omega_0}{M}\alpha P_{w,1}}=\frac{P_{w,1}-P_{w,real}}{P_{w,1}} \quad (26)$$

The relative error index ranges from 0 to 1. It measures the share of deceleration-area overestimation caused by using a single-machine wind model instead of the actual wind farm model, relative to the deceleration area from the single-machine model. It depends only on the wind power representation and is independent of system characteristics and interconnection location. A larger index means a more idealized (overly optimistic) transient-stability assessment; a smaller index means closer agreement with the true stability. At the limit of 1, the single-machine active-power reference is much larger than the actual model's, yielding a pronounced overestimation of the deceleration area and an overly optimistic assessment. At 0, the single machine and actual references совпадают, the deceleration area is accurate, and the assessment reflects the true stability level.

4.3 Wind Farm Equivalencing Based on the Optimal Recovery Rate

The number of turbine units used in a wind farm equivalent model affects the power recovery process and thus system transient stability. To improve the accuracy of transient stability simulation and analysis for power systems with large-scale wind integration while maintaining computational efficiency, this paper models wind farm dynamics with a small number of turbine units whose active power reference outputs are made as consistent as possible with the wind farm's actual output. Accordingly, an recovery rate oriented wind farm equivalencing method is proposed.

4.3.1. Single Machine Equivalent Modeling Method

Since the active power recovery rate of the single unit equivalent wind farm model is fixed, it cannot represent the loss of recovery rate during the active power recovery process, resulting in deviations in the active power output reference values. To address this issue, the single unit model's recovery rate can be optimized to minimize the mismatch in active power reference values, thereby improving the consistency between the equivalent model output and the actual wind farm output.

Common indicators for quantifying the difference between two active power output curves include the mean square error (MSE) and the maximum vertical distance. In this paper, MSE is adopted for the analysis. The MSE is calculated as[26]:

$$MSE = \frac{1}{N}\sum_{i}\left[y_A(x_i) - y_B(x_i)\right]^2 \tag{27}$$

Consider the post fault active power restoration stage in which n turbines within the wind farm are scheduled to participate in coordinated power recovery. Solving the corresponding optimization problem yields the optimal ramp rates for the participating units. For turbine i, the active power recovery rate is denoted by v_i, and the recovery is completed at time t_i.At that moment, the reference value of the wind farm active power output is P_i .

Then, for the stand alone equivalent model, the objective function is given by:

$$\min MSE = \frac{1}{n}\sum_{i=1}^{n}\left[nk'(t_i - t_c) - P_i\right]^2 \tag{28}$$

Under the proposed optimization approach, the recovery rate of the equivalent model that minimizes the mean squared error (MSE) is given by:

$$nk' = \frac{\sum_{i=1}^{n}(t_i - t_c)P_i}{\sum_{i=1}^{n}(t_i - t_c)^2} \tag{29}$$

Accordingly, the optimal active power recovery rate for each unit is given by:

$$k' = \frac{\sum_{i=1}^{n}(t_i - t_c)P_i}{n\sum_{i=1}^{n}(t_i - t_c)^2} \tag{30}$$

At this point, assuming that each unit in the wind farm recovers at its optimal recovery rate, the power reference value of the single-machine equivalent model during the recovery phase can be expressed as follows:

$$P'_{w,1} = \mathrm{n}k'(t - t_c) \tag{31}$$

4.3.2 Multi-Machine Equivalent Modeling Method

When the single machine equivalent model of a wind farm, even with the optimal recovery rate, still fails to satisfy the accuracy requirements of synchronous generator transient stability analysis, the multi machine equivalent method should be considered.

The multi machine equivalence method is based on time segmenting the active power output reference of the actual wind farm and then carrying out the equivalence for each segment separately. Since the equivalence error in each time segment is independent of that in the other segments, the equivalence process within each segment can be treated as a single machine equivalence problem. Moreover, the preceding subsection has already presented the methods for determining the optimal recovery rates of both the wind farm and the turbine in the single machine equivalencing process. Therefore, in the multi machine equivalencing of a wind farm, the key issue is how to determine the optimal partition points based on the wind farm's active power reference and the characteristics of its active power recovery rate.

If the prefault active power output of each unit is known, the time at which each unit completes active power recovery can be determined. According to (21), the wind farm active power output reference and the corresponding recovery rate at each instant can then be obtained, which makes it possible to calculate the decrease in the recovery rate relative to the previous instant. By ranking these decreases in descending order, the instant corresponding to the largest decrease in the recovery rate is selected as the first optimal segmentation point. Subsequently, the single machine equivalent method is applied to each segment sepa-rately to determine the optimal recovery rate, the mean square error, and the overes timation of synchronous generator transient stability. Using the same procedure, the second optimal segmentation point is identified, and the optimal recovery rate, mean square error, and transient stability overestimation for each segment are calculated. This process is repeated until the required accuracy is achieved.

This paper employs an exhaustive search to validate the optimal segmentation points. Within the actual active power restoration interval of the wind farm, candidate first segmentation points are scanned using a specified time step. For each candidate point, the recovery rate, mean square error, and synchronous generator transient stability overestimation are computed for each resulting segment. By comparing the mean square error and transient stability overestimation across all traversed candidates, the instant at which both metrics are minimized is identified as the true first optimal segmentation point. After the first point is determined, the remaining optimal segmentation points are identified in the same manner until the required accuracy is achieved.

In this paper, the flowchart of the wind farm equivalencing method proposed is presented in Figure 3.

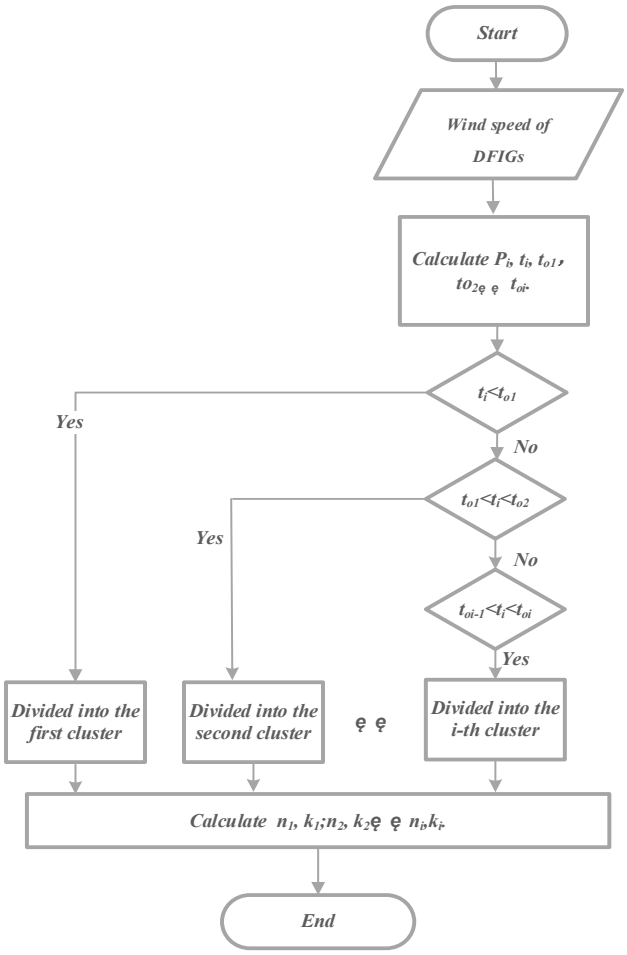

Figure 3. Flowchart of the wind farm equivalent method

5. Case Study

In this paper, the wind turbines are modeled using a fixed pitch active power recovery model. Before the wind turbines were integrated, the outputs of the two generators were 123 MW and 85 MW, respectively.For simulation based validation, both an actual wind farm model comprising 34 turbines and its single machine equivalent model were considered. A synchronous generator of the same rated capacity was used to replace the 123 MW unit. A three-phase short circuit fault was applied at a location 20% of the line length to the right of the PCC, as illustrated in Figure 4 and Figure 5.

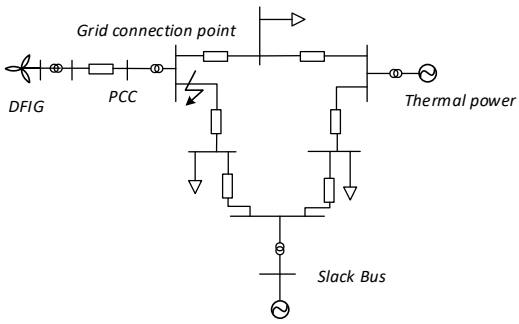

Figure 4. Schematic diagram of the grid connected system with the single machine equivalent wind farm

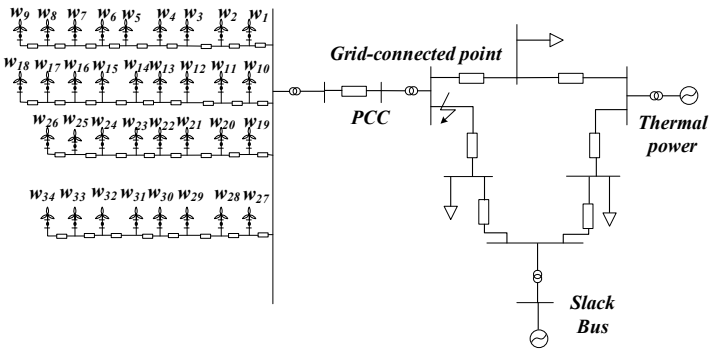

Figure 5. Schematic diagram of the grid connected system with the actual wind farm

As shown in Figs. 4 and 5, the simulation system consists of two main parts. The left hand part represents the wind farm, in which either the detailed 34 turbine model or its single machine equivalent replaces generator G2 in the IEEE 3 machine 9 bus system on an equal capacity basis. Within the wind farm, adjacent turbines are inter-connected by impedance branches. The turbine units are stepped up to the PCC through two step up transformers and are then connected to the grid interconnection point via an additional transformer. The right hand part corresponds to the remainder of the 3 machine 9 bus system, comprising two synchronous generators with their respective step up transformers, transmission lines, and load components.

5.1 Single Machine Equivalence Method

Under the condition that the wind turbine point of interconnection (POI) is fixed at the bus where the original high output thermal unit is connected. The corresponding results are shown in the figure 6. Further more, according to (19), the variation of the second derivative of the synchronous generator rotor angle under different operating conditions can be calculated to characterize the

impact of the wind turbine active power restoration process on the acceleration behavior of the synchronous generator rotor.

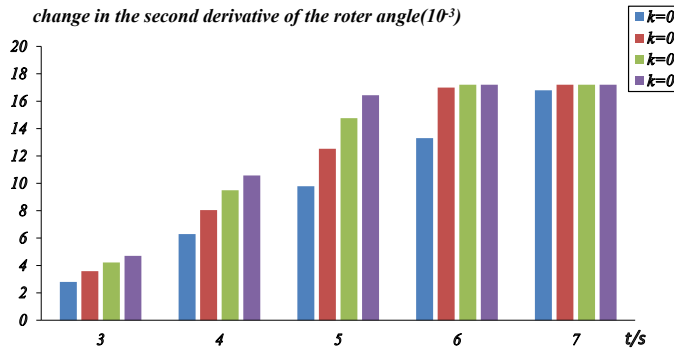

Figure 6. Change in the second derivative of the rotor angle of the synchronous generator

During the wind turbine active power recovery phase, if the recovery rate is fixed, a longer recovery duration implies greater cumulative power support from the turbine, resulting in a larger magnitude of the synchronous generator rotor angle second derivative, which is beneficial for transient stability. For a given recovery duration, the second derivative increases with the active power recovery rate. Therefore, within the system's stable operating range, a higher active power recovery rate is more favorable for enhancing transient stability.

After the recovery phase ends, the active power support provided by the DFIGs becomes constant, and the second derivative of the system rotor angle correspondingly remains constant. Hence, the system's stability becomes independent of the recovery rate, and the simulation results agree well with the theoretical derivation. Moreover, as the recovery rate increases, the rotor angle difference between the synchronous units before and after wind turbine integration decreases, indicating an improvement in system transient stability.

5.2 Multi Machine Equivalencing Method

According to the wind farm equivalencing method proposed in this paper, the optimal recovery rate of the singleunit equivalent model is determined. The maximum decrease in recovery rate is calculated to be 0.013 p.u./s, occurring at t = 3.83 s, which corresponds to the first optimal segmentation point. Subsequently, based on the number of generating units whose recovery time is less than the first optimal segmentation point, the number of units in the second generator group and the corresponding recovery rate are determined, thereby identifying the second optimal segmentation point.With n1=18, k1=0.18 p.u./s, and n2=16, k2=0.16 p.u./s.The corresponding unit grouping results are as follows: the units are classified into two clusters: the first cluster comprises W1, W12-W14, and W21-W34, whereas the second cluster comprises W2-W11 and W15-W20.

By comparing the commonly used single machine equivalent model, the wind farm optimization based theoretical model proposed in this paper, and the detailed 34 unit wind farm model, it is shown that the proposed optimization based model can, to a certain extent, capture the actual wind farm's dynamic behavior more accurately than the conventional single machine equivalent model. As a result, it improves the credibility of transient stability simulations for power systems with DFIGs integration.

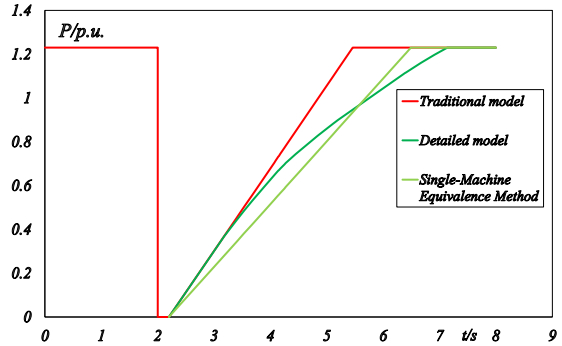

(a) Single Machine Equivalent Model

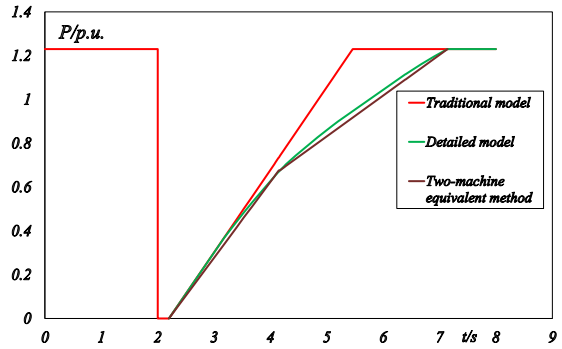

(b) Two Machine Equivalent Model

Figure 7. Simulation Results of Wind Farm Output

In Figure 7, the red curve represents the output of the conventional single machine equivalent model reported in the literature, while the green curve represents the actual wind farm output. The light green and purple curves denote the outputs of the single machine and two-machine equivalent models proposed in this paper, respectively. Compared with the method reported in the literature, the proposed method produces output curves that more closely match the actual wind farm output, and its recovery time is also closer to the actual recovery time of the wind farm.

The model access method proposed in this paper evaluates the discrepancy by calculating the difference between the rotor angle separation of synchronous generators in the benchmark system and that in the system with the actual wind farm connected. In this way, the rotor-angle difference error for different equivalent wind farm models is obtained, as shown in Figure 8.

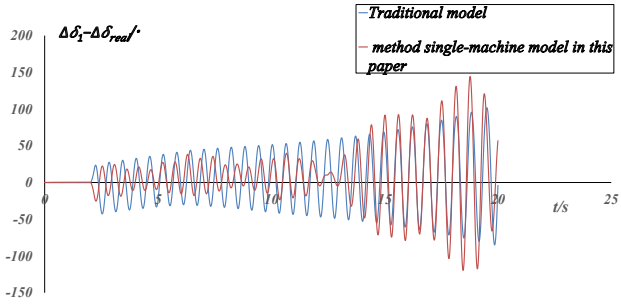

(a)Comparison between the single machine equivalence method and traditional methods

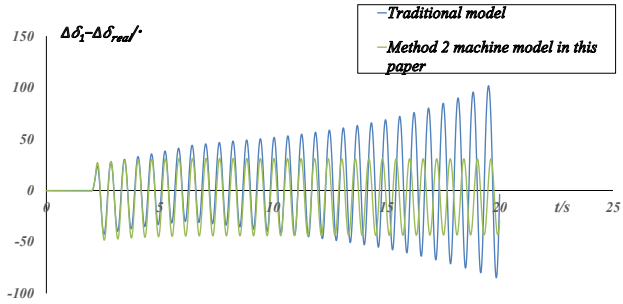

(b) Comparison of the multi machine equivalence method and traditional methods

Figure 8. Error Magnitude of Power Angle Difference

A comparative examination of Figure 8 indicates that both the proposed method and the approach in [21] can be broadly divided into three stages.Stage One (0-2s): Disturbance initiation. At approximately 0 s, the power angle difference is close to 0°. Following the disturbance, it increases rapidly and reaches the first peak of about 20° at around 1 s. It then drops quickly, reaching the first trough of approximately -15° at about 1.5 s.Stage Two (2-8 s): Oscillation damping. The power angle difference exhibits a clear damped oscillatory response with progressively de-creasing amplitude. The second oscillation has a peak of roughly 10° and a trough of about -8°; the third oscillation has a peak of about 5° and a trough of about -4°; and the fourth oscillation has a peak of around 2° and a trough of approximately -2°. The oscillation frequency is relatively high, about 1.5-2 Hz.Stage Three (8-20 s): Stabilization. After roughly 8 s, the oscillation amplitude becomes very small (within ±1°). After about 10 s, the response is essentially stable around 0° and ultimately converges to 0°, indicating that synchronism is restored.

The three stages of the method in reference [21] can be summarized as follows:Stage One (0-2s): Disturbance onset. After the disturbance, the power angle difference increases more rapidly and with a larger amplitude, reaching the first peak of approximately 30° at around 0.8 s.Stage Two (2-10s): Large amplitude oscillation. The oscillation magnitude is greater than that of the method in this paper. The maximum negative swing reaches about -60° to -80°, and the oscillations decay more slowly, indicating weaker damping.Stage Three (10-20s): Slow conver-gence. The response converges slowly; even after about 15 s, fluctuations of approximately ±5° persist, and a slight steady state error remains.

Compared with the method in [21], the single machine and multi machine equivalent methods proposed in this paper produce smaller power angle difference errors. Their responses are closer to those obtained when the detailed wind farm model is connected, and the absolute error remains relatively stable with less fluctuation.

Based on the above results, the transient stability assessment error indices are calculated. Compared with the method in [21], the single machine equivalent method proposed in this paper reduces the absolute error index from 3.9×10^{-3} to 1.58×10^{-3}, while the relative error index decreases from 22.68% to 9.19%. For the two machine equivalent access method proposed in this paper, the absolute error index is 4.04×10^{-3}, and the relative error index is reduced from 22.68% to 2.35%. These results indicate that the equivalent methods proposed in this paper can reflect the dynamic behavior of actual wind farms more accurately, reduce simulation errors caused by inaccurate wind farm modeling, and improve the reliability of transient stability simulation analysis for power systems with wind farm integration.

6. Conclusion

This paper analyzes the influence mechanism of wind turbine active power recovery dynamics on power system transient stability, establishes an analytical model, and systematically evaluates the effect of wind farm recovery rate. The main conclusions are as follows: firstly, in systems integrated with doubly fed wind farms, synchronous generator transient stability depends on generator inertia, wind farm interconnection location, and the mismatch between the equivalent model and actual wind turbine output. Hence, wind farm modeling accuracy directly affects transient stability assessment. Secondly, the single machine equivalent model in this paper improves transient stability assessment accuracy over the conventional single machine equivalent method, but it is more suitable for systems with relatively small synchronous generator inertia and offers limited improvement in long term rotor angle stability analysis of large scale systems. Finally, the proposed multi machine equivalent model has wider applicability and better captures wind farm dynamic behavior during active power recovery, thereby reducing the influence of equivalencing errors on the reliability of transient stability simulation results.

References

[1] Z. Shuai, C. Shen, X. Yin, et al. Fault Behavior Analysis of Inverter-Interfaced Distributed Generators under Different Control Schemes. T-PWRD, 2018, 33(3): 1223-1235.

[2] J. Liu, J. Liu, Y.Wang. Intelligent Enhanced Judgment of Transient Power Angle Stability Based on SBTTC Critical Threshold Adaptive Correction. Proceedings of the CSEE, 2025, 6(5):1765-1779.

[3] D. Chen, C. Li, J. Liu, et al. Analysis of the superposition and attenuation characteristics of transient fault currents in meshed parallel loops containing doubly-fed induction generators. AEPS, 2025, 49(18): 117-126.

[4] Ramadhan A. R., Ali H. R., Irnawan R.. Dynamic State Estimation of aHigh-Order Model of Doubly-Fed Induction Generator Using Unscented KalmanFilter. IEEE Access, 2024, 12: 16344-16353.

[5] Kumar K., Prabhakar, P., Verma A., et al. Advancements in wind power forecasting: A comprehensive review of artificial intelligence-based approaches. Multimed Tools Appl, 2025, 84, 8331-8360.

[6] Z. Guo. Low voltage ride through control strategy and variable-parameter tuning method for doubly-fed induction generators considering wind speed variation. Guangxi University, 2025, 26-32.

[7] Malka L., Kuriqi A., Jurasz J., et al. Strategic selection of wind turbines for low wind speed regions: Impact on cost and environmental benefits. Int. J. Green Energy, 2025, 22(1), 50–71.

[8] T. Gu, Q. Yang, C. Lin, et al. An Equivalent Modeling Method for Wind Farms Based on Single-Machine Equivalence and Mode Selection Analysis. PROT CONTR MOD POW, 2020, 48(1): 102-111.

[9] M. Liu . A Review of Recent Advances in Equivalent Modeling Methods for Wind Farms. ICEPET, Chengdu, China. IEEE, 2024, 79-82.

[10] J. Chen. Research on control parameter identification and wind farm equivalencing methods for doubly-fed wind turbines[D]. Xi'an University of Technology, 2025, 4-6.

[11] Z. Wu, J. Pei, Y. Li. A Multi-Machine Equivalent Method for Doubly-Fed Wind Farms Based on Low Voltage Ride Through Power Characteristics. Autom. Electr. Power Syst., 2022, 46(19):95-103.

[12] X. Zhou, J. Chen. Multi-machine equivalent method for doubly-fed wind farms considering active power recovery characteristics. J. Northeast Electr. Power Univ., 2019, 36(6):1-9.

[13] L. Zheng, K. Jia, T. Bi, et al. Cosine Similarity Based Line Protection for Large Scale Wind Farms. IEEE Trans. Ind. Electron, 2021,68(7): 5990-5999.

[14] J. Zuo, X. Yang, X. Zhao, et al. Multi-Machine Aggregation, Identification, and Equivalent Modeling Method for Direct-Drive Permanent-Magnet Wind Farms Considering LVRT Power Characteristics. PROT CONTR MOD POW, 2025, 53(2): 14-26.

[15] S. Liu, Z. Wang, T. Bi. Multi-Machine Characterization Method for DFIG Wind Power Plants Considering Differences in Rotor Side Converter Control Switching Modes. Autom. Electr. Power Syst., 2023, 47(14):130-139.

[16] Matavalam A. R., Hou B., Choi H., et al. Data-driven transient stability analysis using the Koopman operator. International Journal of Electrical Power & Energy Systems, 2024, 162:110307.

[17] Bogodorova T., Osipov D., Chow J. H., Misclassification Prediction for Transient Stability Assessment, IEEE Transactions on Power Systems, 2024, 39(6): 7429-7432.

[18] Keivanimehr M, Zareian J. M., Chamorro H. R., et al. A Hybrid Method Based on Corrected Kinetic Energy and Statistical Calculation for Real Time Transient Stability Evaluation. Processes. 2024, 12(11): 2409.

[19] H. Peng, Y. Xue, Q. Liu, et al. Case screening for quantitative analysis of power system transient stability under complex models. Autom. Electr. Power Syst., 2025, 49(10): 145-153.

[20] Brik A., Kouba N. E. Y., Ladjici A. A.. Power System Transient Stability Analysis Considering Short-Circuit Faults and Renewable Energy Sources. In The 3rd International Electronic Conference on Processes. MDPI, 2024, 42.

[21] L. Tang, C. Shen, X. Zhang. Impact of Large-Scale Wind Power Integration on Transient Power Angle Stability of Power Systems (Part II): Analysis of Influencing Factors. Proceedings of the CSEE, 2015, 35(16): 4043-4051.

[22] Y. Gu, Y. Zhou. Analysis of the Influence of Active Power Recovery Rate on the Transient Stability Margin of a New-Type Power System, Processes, 2025, 13(7): 2020.

[23] Y. Zhang, M. Ding, P Han, et al. Analysis of the Interactive Effects of DFIG and UHVDC Active Power Recovery Rates on the Rotor Angle Stability of the Sending-End System, IEEE Access, 2019, 7: 79944-79958.

[24] Q. Yang, Y. Sun, Z. Wang, et al. Study of Power Angle and Voltage Dominated Instability Modes in a Synchronous Generator-Wind Power Transmission System Based on Critical Voltage, Energy Reports, 2026, 15: 108902.

[25] S. Wang, X. Zhang, Y. Wang. Inertia Control of DFIG-Based Wind Turbines for Enhancing the Stability of Interconnected Power Systems, ICEMS, Sydney, NSW, Australia, IEEE, 2017: 1-5.

[26] M. Han, H. Zhao, J. Cheng, et al. Real-Time Equivalent Modeling of Wind Farms Based on Wind Speed Forecasting, RPG 2021, IET 2021: 1193-1202.